RESEARCH PAPER

Cancer Biology & Therapy 15:5, 612–622; May 2014; © 2014 Landes Bioscience

Overexpression of DDR2 contributes to cell invasion and migration in head and neck squamous cell carcinoma

Jinke Xu[1,2,3,†], Wei Lu[1,2,†], Senlin Zhang[3,†], Chuchao Zhu[2], Tingting Ren[2], Tong Zhu[2], Hu Zhao[2], Yanpu Liu[1,*], and Jin Su[2,*]

[1]Department of Oral and Maxillofacial Surgery; School of Stomatology; the Fourth Military Medical University; Xi'an, PR China; [2]State Key Laboratory of Cancer Biology; Department of Biochemistry and Molecular Biology; The Fourth Military Medical University; Xi'an, PR China; [3]Department of Oral and Maxillofacial Surgery; Jinling Hospital; Clinical School of Medical College; Nanjing University; Nanjing, PR China

[†]These authors contributed equally to this work.

Keywords: DDR2, HNSCC, tumor metastasis, EMT, hypoxia

Background: Discoidin domain receptor 2 (DDR2) is a unique receptor tyrosine kinase (RTK) that is activated by fibrillar collagens. Although DDR2 contributes to the metastasis of some tumors, its role in head and neck squamous cell carcinoma (HNSCC) remains unknown. The aim of this study was to investigate the expression level, clinical and pathological significance, and biologic function of DDR2 in HNSCC.

Methods: Real-time quantitative PCR, western blot, and immunohistochemical staining were employed to assess the expression levels of DDR2 in HNSCC specimens. Adenovirus-mediated overexpression of DDR2 was used to evaluate its consequences on cell proliferation, invasion, migration, and the process of hypoxia-induced epithelial-mesenchymal transition (EMT). Then nude mouse xenograft and tail vein metastasis models were utilized to validate the in vitro results.

Results: DDR2 was highly expressed in high grade HNSCC tissues and lowly expressed in low grade HNSCC tissues, but absent or rarely expressed in cancer-associated normal tissues. Both the frequency and expression intensity of DDR2 were significantly associated with tumor pathologic stage and lymph node metastasis. In vitro, DDR2 overexpression in HNSCC cells failed to alter cell proliferation but markedly accelerates cell invasion and migration as well as hypoxia-induced EMT. In vivo, elevated expression of DDR2 speeds up the metastasis of HNSCC cells to the lung.

Conclusion: DDR2 plays an important role in HNSCC metastasis, and might be a promising target for future therapies in this type of cancer.

Introduction

Head and neck squamous cell carcinoma (HNSCC) represents approximately 6% of all cancers and about 500000 cases are diagnosed every year.[1] Over the past 20 years, diagnosis and management of HNSCC have improved through combined efforts in surgery, radiotherapy and chemotherapy, but the overall 5-y survival rate for patients is still only 40–50%.[2] The high rate of recurrence of HSNCC and its significant metastatic potential after conventional therapy appear to be major contributing factors for restricted survival of HNSCC patients.[3] Therefore, understanding the molecular cancer pathways of underlying HNSCC metastasis would help to improve the therapy of the disease.

Discoidin domain receptor 2 (DDR2) is a receptor tyrosine kinase (RTK) that can be activated by fibrillar collagens,[4-6] and implicated in several cancer cell behaviors, including VEGF expression, tumor angiogenesis, invasion, and metastasis.[7-9] Matrix metalloproteinases (MMPs) are an important subset of downstream target genes of DDR2 signaling.[10,11] EMT plays an important role in the metastasis of HNSCC by facilitating primary tumor invasion through the basement membrane and migration through the tumor-associated stroma or extracellular matrix (ECM).[12-14] It has been reported that DDR2 is a critical regulator of EMT.[15] Though previous studies have investigated the function of DDR2 in some common tumors, there has not been functional characterization of the potential role of DDR2 in HNSCC. Therefore, the aim of the current study was to investigate this issue.

Results

DDR2 is highly expressed in high-grade HNSCC

In order to explore the role of DDR2 in HNSCC, we first compared its expression levels in non-cancerous and cancer tissues. The results of real-time quantitative PCR (qPCR) showed that the mRNA expression level of DDR2 was much higher in all the tumor tissues than in their normal counterparts, and

*Correspondence to: Yanpu Liu; Email: liuyanpu@fmmu.edu.cn; Jin Su; Email: sujin923@fmmu.edu.cn
Submitted: 01/19/2014; Accepted: 02/10/2014; Published Online: 02/20/2014
http://dx.doi.org/10.4161/cbt.28181

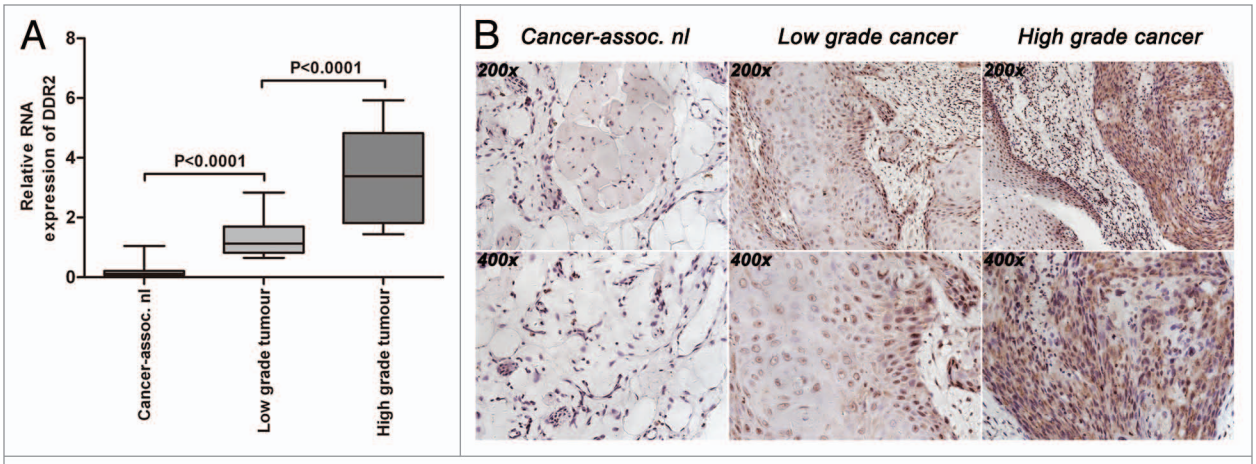

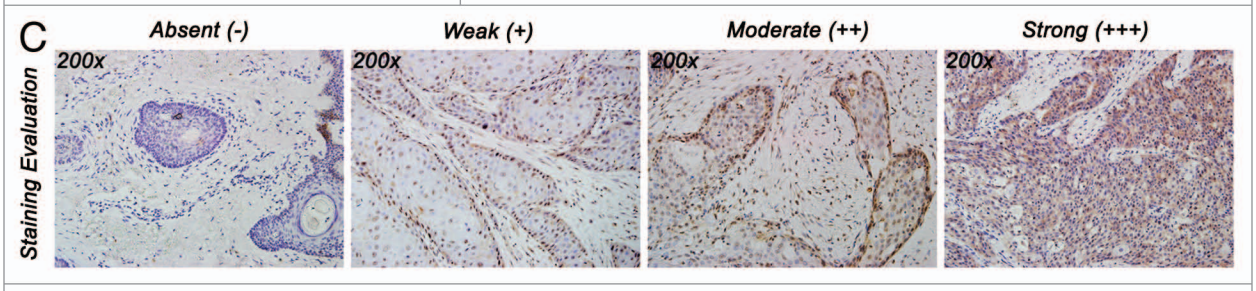

D

Head and neck tissue	DDR2(-)	DDR2(+)	χ^2 value	P
HNSCC	2	77	88.245	<0.005
Cancer-assoc. nl tissue	34	5		

E

Clinicopathological Features		Expression level of DDR2 –	+	++	+++	χ^2 value	P
Genger	Male	2	24	16	8	3.5141	>0.250
	Female	0	19	8	2		
Age	≤60 years	0	27	19	7	6.061	>0.100
	> 60 years	2	16	5	3		
Grade	Low	2	40	12	0	38.361	<0.005
	High	0	3	12	10		
Lymph node Metastasis	(-)	2	41	10	2	34.839	<0.005
	(+)	0	2	14	8		

Figure 1. Expression levels of DDR2 transcripts and proteins in HNSCC clinical specimens. (**A**) Expression levels of DDR2 in 29 pairs of fresh primary HNSCC and corresponding normal clinical specimens were measured by qPCR. One of the low grade tumors' transcripts (number 5) was used for normalization. (**B**) Immunohistochemical staining for DDR2 expression in 79 human HNSCC specimens (54 specimens of low grade tumors and 25 specimens of high grade tumors) and 39 cancer-associated normal (cancer-assoc. nl) specimens. Shown is a representative example of high grade HNSCC sample (right), low grade HNSCC sample (middle) and cancer-associated normal tissue sample (left). (**C**) Staining evaluation for the immunohistochemical staining of DDR2 expression. The staining grade is stratified as absent (-), weak (+), moderate (++), or strong (+++). Shown is a representative example of each grade. (**D**) Statistical analysis for immunohistochemical staining of DDR2 expression between human HNSCC specimens and cancer-associated normal specimens. (**E**) Statistical analysis for the relationship between the immunohistochemical staining of DDR2 expression and HNSCC characteristics. Data are presented as the mean ± SD or *n* (number of samples). Statistical significance was evaluated with the Student *t* test or χ^2 test.

increased with the increase of tumor grade (**Fig. 1A**). Similar results were also observed in DDR2 protein expression, as determined by immunohistochemistry (**Fig. 1B**). The frequency of positive expression of DDR2 protein was 97.5% (77/79) in human HNSCC specimens, but was only 2.5% (2/79) in the corresponding adjacent normal ones (**Fig. 1C and D**). Both the

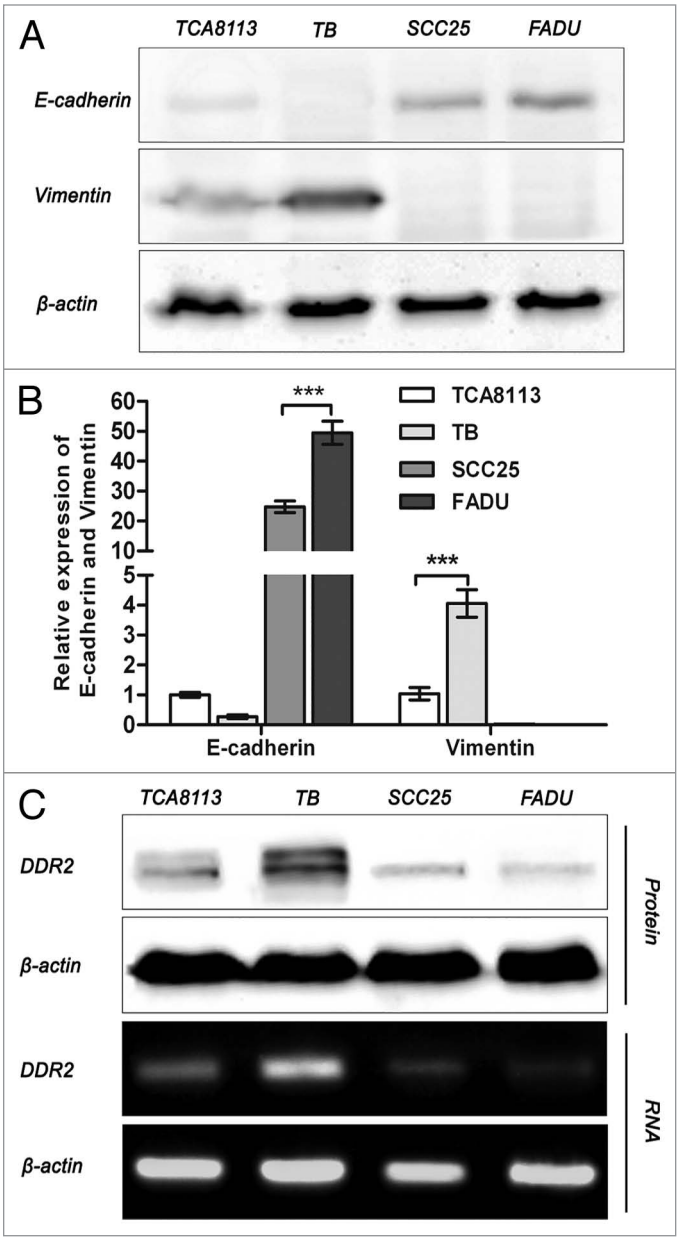

Figure 2. Expression of DDR2, E-cadherin, and vimentin in HNSCC cell lines. (**A and B**) Tca8113, TB, SCC25, and FaDu cells were subjected to analysis of mRNA and protein expression of E-cadherin and vimentin by qPCR and western blot, respectively. Statistical significance was evaluated with the Student *t* test. Results display the mean ± SD. ***$P < 0.001$. (**C**) mRNA and protein expression of DDR2 in HNSCC cell lines was analyzed by reverse transcription PCR and western blot, respectively. β-actin was used as a loading control.

frequency and expression intensity of DDR2 did not correlate with the gender or age of the patients, but were significantly associated with tumor pathologic stage ($\chi^2 = 38.361$, $P < 0.005$) and lymph node metastasis ($\chi^2 = 34.839$, $P < 0.005$) (**Fig. 1E**). These clinical data strongly suggest that DDR2 might be a hallmark of higher tumor grade and metastatic potential of human HNSCC.

DDR2 expression correlates with the metastatic potential of HNSCC cell lines

Clinical evidences indicate that high-grade HNSCC can usually acquire a high metastatic potential that can be marked by the loss of E-cadherin and the expression of vimentin.[16] Thus, the expression levels of DDR2 and the two metastasis markers were analyzed in four human HNSCC cell lines by qPCR and western blot, respectively. Compared with Tca8113 and TB cells, SCC25 and FaDu cells expressed higher level of E-cadherin but had undetectable vimentin (**Fig. 2A and B**). This is consistent with previous descriptions of the phenotypes of these cells,[17] indicating that Tca8113 and TB cells had a metastatic feature, whereas SCC25 and FaDu cells tended to be epithelial-like. DDR2 expression levels was higher in Tca8113 and TB cells than in SCC25 and FaDu cells (**Fig. 2C**), suggesting a direct correlation of DDR2 expression with the metastatic potential of HNSCC cells. Considering that Tca8113 and FaDu cells were more widely used in previous studies than the other two cell lines, they were chosen as our major cell models in the following experiments.

DDR2 overexpression in HNSCC cells fails to alter cell proliferation but markedly enhances cell invasion and migration

To fully understand how DDR2 affects the behaviors of HNSCC cells, we observed the impacts of DDR2 overexpression on cell proliferation, invasion and migration. Tca8113 and FaDu cells were infected with adenovirus expressing either enhanced green fluorescent protein (EGFP) or human DDR2, and the transduced cells were then subjected to cell proliferation assay by MTT and EdU incorporation as well as cell cycle analysis by flow cytometry. The transduction of Ad-DDR2, albeit caused a sharp elevation of DDR2 expression (**Fig. 3A**), had no significant influence on cell proliferation and cell cycle in both cell lines (**Fig. 3B–D**; **Fig. S1**).

Subsequently, we further performed in vitro migration and invasion assays by use of transwell chamber system. It was demonstrated that no significant differences between the mock-transduced cells and parental cells could be observed. In contrast, the DDR2-transduced groups displayed higher capability of invasion and migration than control groups. The promoting effect of DDR2 on these cell functions was amplified by the addition of collagen type I, a well-defined ligand to induce DDR2 activation (**Fig. 4A and B**). As tumor cell invasion on Matrigel-coated surface is partially dependent of the secretion of MMP-2 and MMP-9, we conducted immunoblot to examine their protein levels. It was shown that enhanced expression of DDR2 remarkably boosted the expression of both MMP-2 and MMP-9 (**Fig. 4C**). In addition, we also found that DDR2 knockdown by specific siRNA in TB cells, a cell line with relatively high level of endogenous DDR2, inhibited cell invasion and migration (**Fig. S2**). From these data, it is supposed that the biological consequence of DDR2 in HNSCC cells might predominantly be advancement of tumor invasion and metastasis.

DDR2 controls the process of hypoxia-induced EMT in HNSCC cells

Growing evidences indicate that DDR2 is a mesenchymal marker and a critical regulator of EMT, a process that

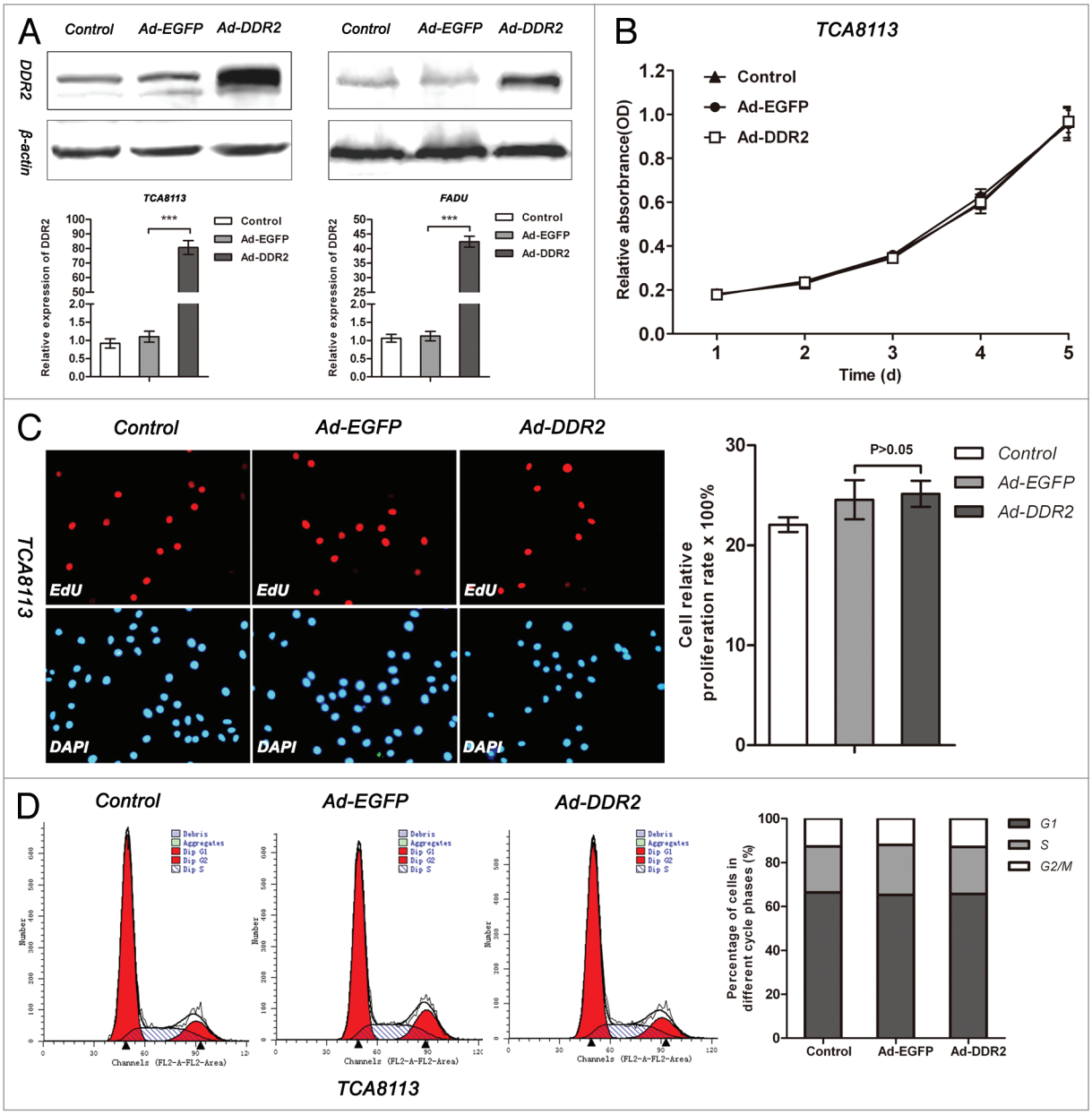

Figure 3. DDR2 overexpression has no effect on cell proliferation in HNSCC cells. (**A**) Tca8113 and FaDu cells (parental, EGFP-, and DDR2-transduced) were cultured in serum-free medium for 24 h. Thereafter, protein and RNA from these cells were extracted and analyzed for DDR2 expression using western blot and qPCR. (**B**) The cell growth curves of Tca8113 cells (parental, EGFP-, and DDR2-transduced) by MTT method. (**C**) Tca8113 cells (parental, EGFP-, and DDR2-transduced) treated by EdU were viewed and photographed using a fluorescence microscope. The staining positive rate was counted as positive cells/overall cells × 100%. For each group, ten random high-power fields (400×) were chosen and the cell number was counted at least three times. The histogram represents the staining positive rate of each group. (**D**) Tca8113 cells infected with Ad-DDR2 were similar to the controls by FAC assays. Statistical significance was evaluated with the Student *t* test. Results display the mean ± SD. ***$P < 0.001$.

mediates tumor progression, including local invasion, spreading through the circulation and metastasis.[18] These established concepts prompted us to investigate whether DDR2 is involved in the phenotypic changes of EMT in HNSCC cells as well. Compared with control cells, the Tca8113 and FaDu cells with ectopic expression of DDR2 did not display obvious changes in either morphology, or the expression levels of EMT marker proteins, including E-cadherin and vimentin (**Fig. 5A–C**, left).

Figure 4 (See next page). Overexpression of DDR2 enhances the invasion and migration in HNSCC cells. (**A and B**) Tca8113 and FaDu cells (parental, EGFP-, and DDR2-transduced) were incubated in serum-free medium with or without 2 μg/mL type I collagen (Col I) for 24 h. The histogram represents the average number of invaded and migrated cells in five random low-power fields (200×). The numbers from the control groups were used as control. Statistical significance was evaluated with the Student *t* test. Results display the mean ± SD. ***$P < 0.001$. (**C**) The cells in (**A**) were subjected to analysis of protein expression of MMP-2 and MMP-9 using western blot.

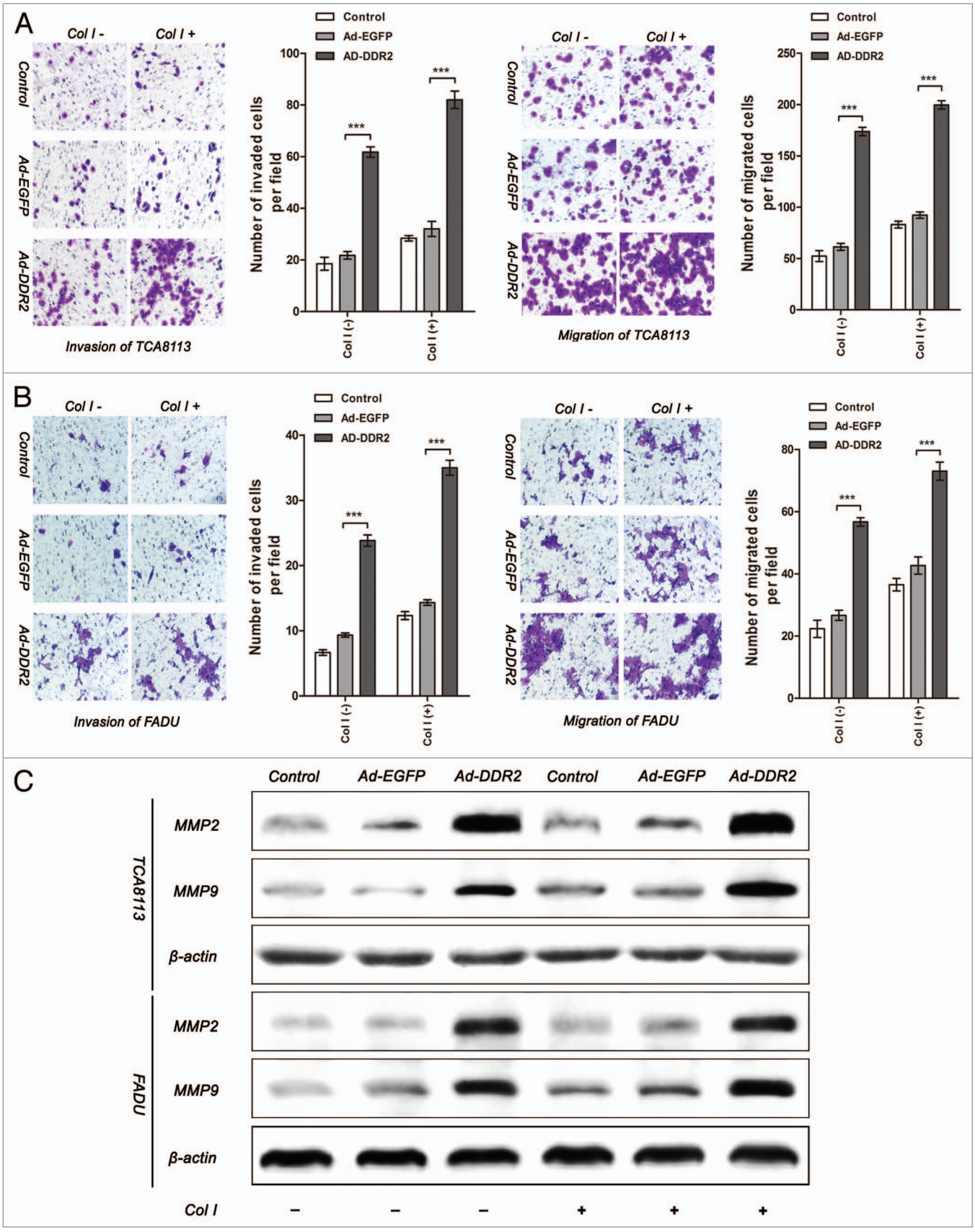

Figure 4. For figure legend, see page 615.

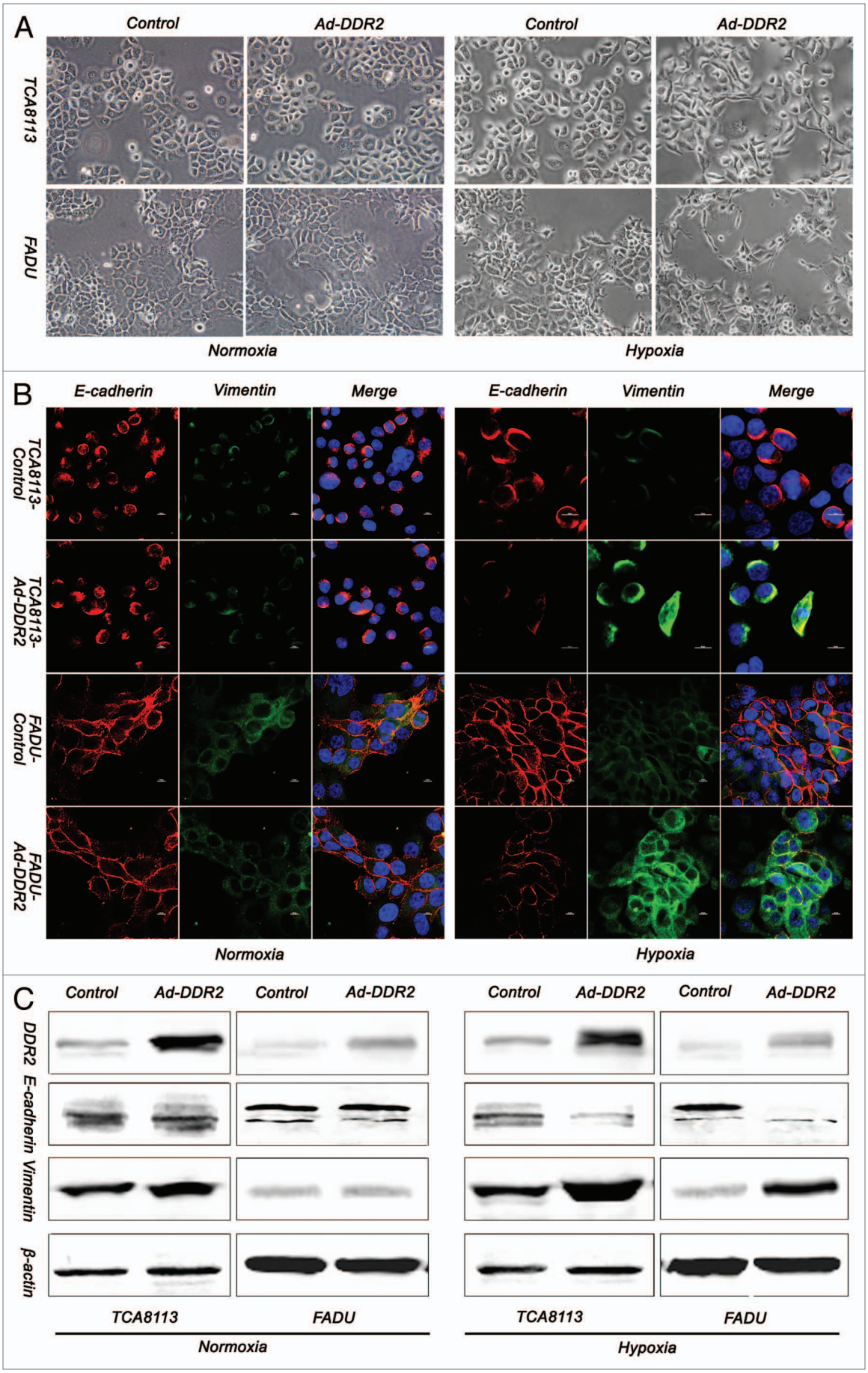

Figure 5 (See previous page). Overexpression of DDR2 accelerates the process of hypoxia-induced EMT in HNSCC cells. (**A**) Tca8113 and FaDu cells (parental and DDR2-transduced) were cultured under normoxic or hypoxic condition for 48 h, and the morphology change of cells were photographed in low-power field (200×). (**B**) The cells in (**A**) were stained for the expression of E-cadherin (red) and vimentin (green) by immunocytofluorescence. Nuclei are labeled by DAPI (blue). Scale bar 10 μm. (**C**) The cells in (**A**) were used for immunoblot analysis of E-cadherin and vimentin expression.

Because hypoxia is a major trigger of tumor cell EMT and metastasis in an in vivo environment, we therefore attempted to observe whether DDR2 participates in EMT of HNSCC cells under low oxygen conditions. As assessed by morphological examination, both Tca8113 and FaDu cells tended to have a spindle-shaped, fibroblastic-like phenotype when were exposed to hypoxic challenge. These hypoxia-induced changes were exaggerated by the introduction of DDR2 into the cells (**Fig. 5A**, right). Further analysis by immunofluorescence and immunoblot revealed that DDR2 reduced E-cadherin expression but increased the expression of vimentin (**Fig. 5B and C**, right). Based on these data, we speculate that the role of DDR2 in EMT of HNSCC cells might be partially dependent on the hypoxic tumor environment.

Elevation of DDR2 expression in human tongue cancer cells speeds up tumor cell metastasis to the lung

Nextly, we tried to determine whether the in vitro effects of DDR2 on HNSCC cell behaviors could be reproduced in vivo. To this end, we utilized human tongue cancer cell line Tca8113 to establish subcutaneous xenograft and tail vein metastasis models in nude mice. Subcutaneous xenograft tumor size among parental, EGFP-, and DDR2-transduced cells did not reveal significant difference across the measurement periods, implying that DDR2 expression has no effect on in vivo tumor growth (**Fig. 6A**).

Because lung is the first capillary bed that tumor cells will encounter following tail vein injections, we assessed the role of DDR2 in Tca8113 cell lung metastasis. It was found that the DDR2-overexpressing Tca8113 cells generated approximately 3-fold more metastases on the lung surface and 5-fold more in the lung than control and EGFP-expressing cells (**Fig. 6B and C**). In addition, the tumor nodules derived from DDR2-transduced cells had enhanced immunoreactivity of both MMP-2 and MMP-9 compared with those from EGFP-transduced group (**Fig. 6D and E**), as demonstrated by histological analysis of the lung tissue sections.

Discussion

HNSCC is characterized by a marked propensity for local invasion and cervical lymph node metastasis.[19] The major fatal complications of HNSCC are tumor recurrence and metastases,[20] which have made patients' care and prognosis challengeable. Therefore, establishment of novel therapeutic approaches against HNSCC metastasis are urgently needed. DDR2 is a candidate tumor promoter gene which regulates cell adhesion, invasion and migration as well as extracellular matrix remodeling. Here our study showed that DDR2 expression level in HNSCC was positively correlated with tumor pathologic stage. Enforced expression of DDR2 in HNSCC cells, albeit failed to alter cell proliferation, markedly enhances cell invasion and migration abilities both in vitro and in vivo.

A notable finding in this study is that high-grade clinical HNSCC specimens express higher level of DDR2 than low-grade ones. Furthermore, both the frequency and expression intensity of DDR2 did not correlate with the gender or age of the patients, but were significantly associated with tumor pathologic stage and lymph node metastasis. Chua et al. reported that DDR2 expression in both primary and metastatic tissues of nasopharyngeal carcinoma (NPC) was significantly higher than in other HNSCC and nasopharyngeal lymphoid hyperplasia tissues.[21] This is consistent with the conclusion from our current study since 98% of the NPC specimens are high-grade cases.[22] Therefore, it is supposed that DDR2 might act as a hallmark of high-grade and metastatic HNSCC.

In addition to these valuable clinical evidences, our in vitro and in vivo data also demonstrated that the role of DDR2 in HNSCC cells is control of cell invasion and metastasis rather than cell proliferation. A series of previous studies indicated that DDR2 plays an important role in regulating cell proliferation.[23-26] However, it was reported that DDR2 did not affect smooth muscle cell proliferation in response to its cognate ligand type I collagen.[27] Up to present, it still remains poorly understood whether DDR2 exerts impact on the proliferative potential of cancer cells. Our data strongly suggest that endogenous DDR2 may not be required for HNSCC cell hyperplasy.

The promoting role of DDR2 in HNSCC cell invasion and metastasis supports the early findings obtained in breast cancer and melanoma.[7-8] Increased expression and activity of MMPs, particularly membrane type MMP-2 and MMP-9, has been documented in HNSCC and was associated with tumor metastasis and poor prognosis.[28-31] We provided evidence that DDR2-overexpressing HNSCC cells exhibited significant increase in the expression of the two MMPs compared with parental cells. In addition, the tumor nodules derived from DDR2-transduced cells had enhanced immunoreactivity of both MMP-2 and MMP-9 compared with those from EGFP-transduced group. Thus, it can be envisaged that DDR2 may promote the invasion and metastasis of HNSCC cells partially through regulation of the expression of MMP-2 and MMP-9.

We also investigated the role of DDR2 in EMT, a critical process contributing to tumor cell metastasis. The results indicated that under hypoxic conditions DDR2-expressing adenovirus had a stronger effect on induction of an EMT-like phenotype than EGFP control. However, DDR2 did not display obvious changes as above under normoxic conditions, suggesting that the role of DDR2 in HNSCC cell EMT might be partially dependent on the hypoxic tumor environment. Several previous experiments showed EMT facilitated primary tumor invasion and metastasis.[32-35] And recent data suggested that during EMT, tumor cells seem to acquire more aggressive traits, and have an increased ability to invade into the surrounding tissues and migrate into the bloodstream.[36] These results suggest that DDR2 could promote HNSCC cell invasion

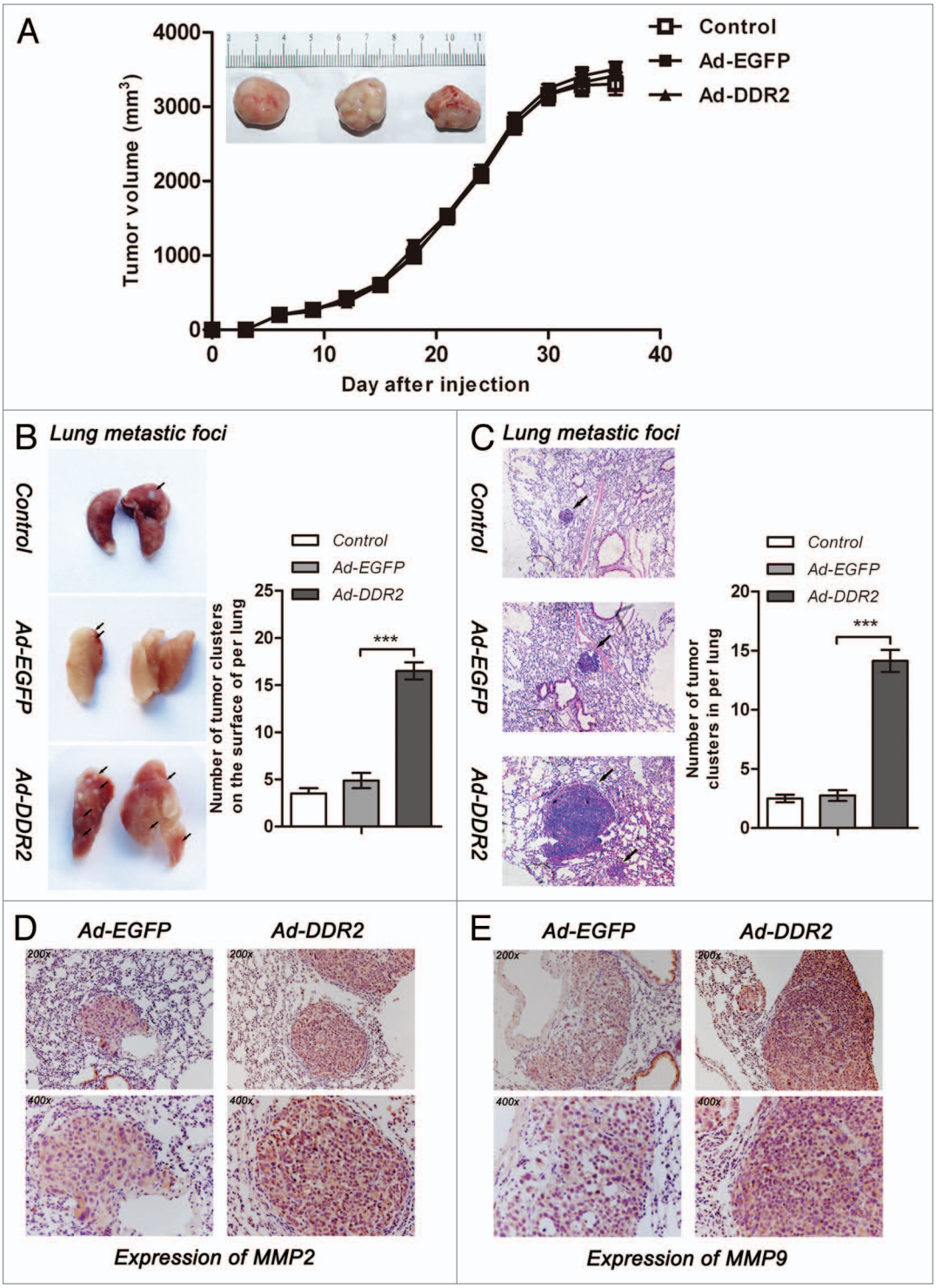

Figure 6. DDR2 enhances the metastasis potential of HNSCC cells in vivo. Tca8113 cells (parental, EGFP-, and DDR2-transduced) (2×10^6/200 μL PBS) were simultaneously injected via the tail veins and subcutaneously into the hind legs of the 6-wk-old female nude mice. At day 42, mice were killed and the lungs were fixed in 4% formaldehyde for 24 h. (**A**) Tumor growth curve. The tumor growth was assessed every 3 d until day 42 by measuring two perpendicular diameters and calculating the volume in mm^3. The typical photographs of tumors are shown. (**B**) The white colonies on the lung surface were enumerated macroscopically. Black arrows indicate lung metastatic tumors. Colonies were enumerated and the relative increases compared with the control groups were calculated. (**C**) Representative lung tissue sections from each group are shown (H&E; original magnification 100×). Black arrows indicate lung metastatic tumors. The number of lung metastatic foci in each group ($n = 4$) was calculated. (**D and E**) Immunostaining of MMP-2 and MMP-9 were performed on lung metastatic tumors (original magnification 200× and 400×). Shown are representative examples from EGFP- and DDR2-transduced groups. Statistical significance was evaluated with the Student *t* test. Results display the mean ± SD .***$P < 0.001$.

and dissemination to the peripheral blood through EMT induction when the cells are encountered with low oxygen supply.

In conclusion, we have disclosed an oncogenic role of DDR2 in the invasion and metastasis of HNSCC. Since HNSCC is characterized by a marked propensity for local invasion and cervical lymph node metastasis, DDR2 may represent a promising therapeutic target for HNSCC. However, more investigations are still needed to elucidate further the mechanism underlying DDR2 control of HNSCC cell metastasis. Research in this direction will finally provide new methods for early diagnosis, novel therapy, and postoperative monitor in HNSCC.

Materials and Methods

Clinical HNSCC specimens

Twenty-nine pairs of fresh primary HNSCC (11 tongue cancers, 3 oropharyngeal cancers, 4 oral floor cancers, 4 lip cancers, 4 gingiva cancers, and 3 buccal mucosa cancers) and corresponding normal samples were obtained from patients with HNSCC in Department of Oral and Maxillofacial Surgery, School of Stomatology, the Fourth Military Medical University (Xi'an, PR China) from 2011 to 2013. The samples considered normal were free of cancer cells by pathologic examination. The patients were classified according to the 2002 Union for International Cancer Control TNM staging criteria[37] before treatment. Written consent of tissue donation for research purposes was obtained from each patient before tissue collection. The protocol was approved by the Institutional Review Board of Fourth Military Medical University. Several HNSCC tissue chips were purchased from Alenabio Corporation (OR601a, Alenabio Co.) which contained 50 HNSCC and 10 normal samples per piece.

Cell lines and reagents

HNSCC cell lines Tca8113 and TB were obtained from the Department of Oral and Maxillofacial Surgery, School of Stomatology, the Fourth Military Medical University; SCC-25 and FaDu were obtained from the American Type Culture Collection (ATCC). All cell lines were cultured according to their directions and guidelines. The cells were maintained at 37 °C in a humidified atmosphere containing 5% CO_2. Before experiments, cells were cultured in serum-free medium for 18 to 24 h. The obtained cell suspension was centrifuged to remove cell debris and suspended in fresh medium to a final concentration of 10^6 cells/ml. For hypoxia treatment, cells were cultured under hypoxic conditions (1% O_2, 5% CO_2, and 94% N_2) and harvested 48 h later. Anti-DDR2 (MMB2538 and BAF2538) antibodies were purchased from R&D Corporation (R&D), anti-E-cadherin (ab11512, Abcam), anti-vimentin, anti-β-actin, anti-MMP-2, and anti-MMP-9 (Cell Signaling). Adenovirus-expressing DDR2 were obtained from Vector Gene Technology Company.

Gene infection and gene transfection

A multiplicity of infection (MOI) of 40 was determined experimentally for Tca8113 and FaDu cells. Cells were seeded in 6-well plates at a density of 5×10^5 cells/well and incubated to reach approximately 80% confluence. After removing the medium, adenovirus-expressing DDR2 (Ad-DDR2) or the negative control gene EGFP (Ad-EGFP) was added in serum-free RAPI1640 or MEM, incubated for 3 h, and then equal amount of fresh culture medium supplemented with 10% FBS was added and incubated for another 24 h.

TB cells were seeded in 6-well plates at a density of 5×10^5 cells/well and incubated to reach approximately 60% confluence. The gene transfection assay was performed with the following constructs using Lipofectamine 2000 (Invitrogen) according to the manufacturer's instructions: a small interfering RNA (siRNA) that targeted human DDR2 (sense sequence: 5′-CCAUGUACAA GAUCAAUUA-3′) and its negative control (NC) siRNA (sense sequence: 5′-UUCUCCGAAC GUGUCACGUT T-3′) (RiboBio Co.). Cells were transfected with siRNA for 6 h and the medium was replaced with RIPA1640 containing 10% FBS until the cells were collected for analysis 48 h later.

Reverse transcription PCR (RT-PCR) and qPCR

Total RNA (500 ng) extracted from cells or tissues with Trizol reagent (Invitrogen, Life Technologies) was converted into cDNA using an AMV reverse transcriptase (Takara Bio) according to the manufacturer's instructions. The primers sequences for PCR amplification were as follows: DDR2, 5′-CTCCCAGAAT TTGCTCCAG-3′ (sense) and 5′-GCCACATCTT TTCCTGAGA-3′ (antisense); E-cadherin, 5′-GTCATCCAAC GGGAATGCA-3′ (sense) and 5′-TGATCGGTTA CCGTGATCAA AA-3′ (antisense); vimentin, 5′-GACAGGATGT TGACAATGCG-3′ (sense) and 5′-GCTGTTCCTG AATCTGAGCC-3′ (antisense); β-actin, 5′-AATCTGGCAC CACACCTTCT ACAA-3′ (sense) and 5′-TAGCACAGCC TGGATAGCAA CG-3′ (antisense). For RT-PCR, the mixture (25 μL) containing a Taq polymerase from Promega was denatured at 94 °C for 5 min, followed by 40 cycles of 94 °C for 30 s, 60 °C for 30 s and 72 °C for 30 s, with a final extension at 72 °C for 10 min. The PCR products were separated in 3% agarose gels by electrophoresis and visualized with ethidium bromide under a UV light. For qPCR, the amplification program was performed by CFX96 Touch PCR system (Bio-Rad). The relative expression levels were normalized using the comparative threshold cycle ($2^{-\Delta\Delta Ct}$).

Western blot

An equal amount of protein extracts (20 μg) were subjected to 10% sodium dodecylsulfate-polyacrylamide gel electrophoresis (SDS-PAGE) and transferred onto nitrocellulose (NC) membranes (Amersham). Subsequently, the NC membranes were blocked with 5% non-fat milk for 1 h at room temperature and then incubated with primary antibodies (1:1000) overnight at 4 °C. After washing three times, the transferred blots were visualized with horseradish-peroxidase (HRP)-conjugated streptavidin or anti-mouse or anti-rabbit secondary antibody (dilution 1:10000, Santa Cruz) for 1 h at room temperature. The enhanced chemiluminescence (ECL) system detection solutions (Pierce) were then applied.

Cell growth tests in vitro

This test includes MTT, EdU incorporation, and flow cytometric analysis (FCA). All the assays were repeated at least three times independently.

MTT assay

Cells were grown in exponential phase and detached by trypsin treatment. Viable cells (2000 cells/ml) were inoculated into

96-well plates and each group had 6 reduplicative wells. At different time points, 20 μL of MTT reagent (5 mg/ml) was added to each well and incubated with the cells at 37 °C for 4 h. The reaction was stopped by the addition of 150 μL dimethyl sulfoxide (DMSO) followed by shaking for 10 min. Absorbance (A) values were measured with an autokinetic enzyme scaling meter (Bio-Rad) at 490 nm wavelength. Cell growth curves then were plotted based on the average A values.

EdU assay

After removing culture medium from the 96-well plates, 100 μL EdU (50 μM, 1: 1000, RiboBio Co.) were added into each well and subsequently incubated for 2 h. After washing, the cells were fixed using 4% buffered formaldehyde for 30 min. The cells were cultured in 4% glycine for 5 min. After washing with PBS, the cells were permeabilized with 0.5% Triton X-100 for 5 min followed by washing with PBS. The cells were then stained with Apollo staining reagent (100 μL) and incubated for 30 min. After permeabilization for 30 min, the cells were washed with 100 μL methanol, followed by washing with PBS. The cells were then incubated with 100 μL 4'6-diamidino-2-phenylindole (DAPI) for 30 min. After washing with PBS, the wells were viewed and photographed using a fluorescence microscope. The staining positive rate was counted as positive cells/overall cells × 100%. For each sample, the cell number was counted at least three times.

FCA

After incubated with serum-free substratum for 48 h, cells were collected, centrifuged and fixed in 95% ethanol. After overnight incubation at 4 °C, cells were stained with 0.5% propidiumiodide (10 μL) in the presence of 0.01% RNase A and 0.1% Triton X-100, and then analyzed with a flow cytometer.

In vitro migration and invasion assays

Invasion assay with a Matrigel-coated membrane and migration assay with no Matrigel membrane were performed using a 24-well transwell inserts (8 μm pore filters, BD Biosciences) according to the manufacturers' instructions. The exponential phase cells were harvested and resuspended (5×10^5 cells/ml) in serum-free medium, and then seeded in the upper chamber. Culture medium with 20% FBS was placed in the bottom well. The transwell chambers were incubated at 37 °C and 5% CO_2 atmosphere for 24 h. The Tca8113 and FaDu cells were allowed to migrate through a porous to the bottom of the membrane. After incubation, the cells on the bottom of the membrane were fixed with 4% paraform for 30 min and then stained with 0.025% Crystal violet. The numbers of invaded cells or migrated cells were determined by microscope at a 200× magnification on each membrane and calculated the mean number of cells per field.

Nude mice subcutaneous xenograft and tail vein metastasis models

Six-week-old nude mice were purchased from Shanghai Experimental Center (CSA). All the experimental procedures were conducted in accordance with the Detailed Rules for the Administration of Animal Experiments for Medical Research. All efforts were made to minimize the animals' suffering and to reduce the number of animals used.

Before the experiment, Tca8113 cells (parental, EGFP- and DDR2-transduced) were incubated with serum-free substratum for 24 h. The female nude mice were randomly divided into three groups ($n = 4$ for each group). Then the cells (2×10^6 cells/0.2 mL PBS) were simultaneously injected via the tail veins and subcutaneously into the hind legs of the mice (day 0). Tumors were measured (perpendicular diameters) every 3 d and their volumes were calculated. Six weeks later, mice were killed for evaluation of tumor size and lung metastasis. The number of Tca8113 colonies present on the surface of each lung was determined by a visual inspection and the lung metastases were confirmed by H&E staining.

Immunohistochemistry and immunocytofluorescence staining

Immunohistochemical and immunocytofluorescence staining was performed to assess the protein expression of DDR2, E-cadherin, vimentin, MMP-2, and MMP-9. For immunohistochemistry, formalin-fixed tumor tissues were embedded in paraffin, and serial sections (4 μm) were dewaxed in toluene, rehydrated in an alcohol gradient, permeabilized in citrate buffer (pH 6.0), quenched with 3% H_2O_2 for 5 min to eliminate endogenous peroxidase activity, washed in PBS, incubated with first antibodies overnight and then with biotinylated goat anti-mouse or anti-rabbit IgG antibody for 15 min. After washing, sections were incubated with streptavidin–peroxidase, lightly counterstained with hematoxylin, and observed under a photomicroscope.

For immunocytofluorescence, cells grown on glass coverslips were fixed with ice-cold 4% paraformaldehyde for 15 min at –20 °C, followed by permeabilization with 0.3% Triton X-100. The cells were incubated with anti-E-cadherin and anti-vimentin (1:100) antibodies at 4 °C overnight, followed by incubation with a mixture of two secondary antibodies conjugated to fluorescein isothiocyanate (FITC) and indocalfaocyanines 3 (CY3). The nuclei were counterstained with 4'6-diamidino-2-phenylindole (DAPI) and observations were performed with a confocal microscope (Leica SP1 and SP2 UV; Leica)

Staining evaluation

An immunoreactivity score system based on the proportion and intensity of positively stained cancer cells was applied. The extensional standards taken were as follows: (1) number of positive stained cells ≤5%, scored 0; 6–25%, scored 1; 25–50%, scored 2; 51–75%, scored 3; and >75%, scored 4; and (2) intensity of stain: colorless, scored 0; pallideflavens, scored 1; yellow scored 2; and brown, scored 3. The extensional standards (1) and (2) were multiplied, and the staining grade was stratified as absent (0 score), weak (1–4 score), moderate (5–8 score) or strong (9–12 score). Specimens were rescored if the difference of scores from the 2 pathologists was greater than 3. Tumors with moderate or strong immunostaining were classified as having high expression, whereas tumors with absent or weak immunostaining were classified as having low expression.

Statistical analysis

SPSS 13.0 software was used to perform statistical analyses. Data are presented as the mean ± SD or n (number of samples), and statistical comparisons were made using χ^2 test or one-way ANOVA followed by the Student t test. $P < 0.05$ was considered statistically significant.

Disclosure of Potential Conflicts of Interest

No potential conflicts of interest were disclosed.

Acknowledgements

This work was supported by the Chinese National Key Basic Research and Development Program (2010CB529705) and grants from National Natural Science Foundation of China (81070820, 81372389).

Supplemental Materials

Supplemental materials may be found here:
www.landesbioscience.com/journals/cbt/article/28181

References

1. Jemal A, Siegel R, Xu J, Ward E. Cancer statistics, 2010. CA Cancer J Clin 2010; 60:277-300; PMID:20610543; http://dx.doi.org/10.3322/caac.20073
2. Haddad RI, Shin DM. Recent advances in head and neck cancer. N Engl J Med 2008; 359:1143-54; PMID:18784104
3. Leemans CR, Braakhuis BJ, Brakenhoff RH. The molecular biology of head and neck cancer. Nat Rev Cancer 2011; 11:9-22; PMID:21160525; http://dx.doi.org/10.1038/nrc2982
4. Ichikawa O, Osawa M, Nishida N, Goshima N, Nomura N, Shimada I. Structural basis of the collagen-binding mode of discoidin domain receptor 2. EMBO J 2007; 26:4168-76; PMID:17703188; http://dx.doi.org/10.1038/sj.emboj.7601833
5. Vogel WF, Abdulhussein R, Ford CE. Sensing extracellular matrix: an update on discoidin domain receptor function. Cell Signal 2006; 18:1108-16; PMID:16626936; http://dx.doi.org/10.1016/j.cellsig.2006.02.012
6. Leitinger B, Kwan AP. The discoidin domain receptor DDR2 is a receptor for type X collagen. Matrix Biol 2006; 25:355-64; PMID:16806867; http://dx.doi.org/10.1016/j.matbio.2006.05.006
7. Badiola I, Villacé P, Basaldua I, Olaso E. Downregulation of discoidin domain receptor 2 in A375 human melanoma cells reduces its experimental liver metastasis ability. Oncol Rep 2011; 26:971-8; PMID:21701781
8. Zhang K, Corsa CA, Ponik SM, Prior JL, Piwnica-Worms D, Eliceiri KW, Keely PJ, Longmore GD. The collagen receptor discoidin domain receptor 2 stabilizes SNAIL1 to facilitate breast cancer metastasis. Nat Cell Biol 2013; 15:677-87; PMID:23644467; http://dx.doi.org/10.1038/ncb2743
9. Valiathan RR, Marco M, Leitinger B, Kleer CG, Fridman R. Discoidin domain receptor tyrosine kinases: new players in cancer progression. Cancer Metastasis Rev 2012; 31:295-321; PMID:22366781; http://dx.doi.org/10.1007/s10555-012-9346-z
10. Olaso E, Ikeda K, Eng FJ, Xu L, Wang LH, Lin HC, Friedman SL. DDR2 receptor promotes MMP-2-mediated proliferation and invasion by hepatic stellate cells. J Clin Invest 2001; 108:1369-78; PMID:11696582; http://dx.doi.org/10.1172/JCI200112373
11. Labrador JP, Azcoitia V, Tuckermann J, Lin C, Olaso E, Mañes S, Brückner K, Goergen JL, Lemke G, Yancopoulos G, et al. The collagen receptor DDR2 regulates proliferation and its elimination leads to dwarfism. EMBO Rep 2001; 2:446-52; PMID:11375938; http://dx.doi.org/10.1093/embo-reports/kve094
12. Masui T, Ota I, Yook JI, Mikami S, Yane K, Yamanaka T, Hosoi H. Snail-induced epithelial-mesenchymal transition promotes cancer stem cell-like phenotype in head and neck cancer cells. Int J Oncol 2014; 44:693-9; PMID:24365974
13. Way TD, Huang JT, Chou CH, Huang CH, Yang MH, Ho CT. Emodin represses TWIST1-induced epithelial-mesenchymal transitions in head and neck squamous cell carcinoma cells by inhibiting the β-catenin and Akt pathways. Eur J Cancer 2014; 50:366-78; PMID:24157255; http://dx.doi.org/10.1016/j.ejca.2013.09.025
14. Thiery JP, Acloque H, Huang RYJ, Nieto MA. Epithelial-mesenchymal transitions in development and disease. Cell 2009; 139:871-90; PMID:19945376; http://dx.doi.org/10.1016/j.cell.2009.11.007
15. Walsh LA, Nawshad A, Medici D. Discoidin domain receptor 2 is a critical regulator of epithelial-mesenchymal transition. Matrix Biol 2011; 30:243-7; PMID:21477649; http://dx.doi.org/10.1016/j.matbio.2011.03.007
16. Onder TT, Gupta PB, Mani SA, Yang J, Lander ES, Weinberg RA. Loss of E-cadherin promotes metastasis via multiple downstream transcriptional pathways. Cancer Res 2008; 68:3645-54; PMID:18483246; http://dx.doi.org/10.1158/0008-5472.CAN-07-2938
17. Christiansen JJ, Rajasekaran AK. Reassessing epithelial to mesenchymal transition as a prerequisite for carcinoma invasion and metastasis. Cancer Res 2006; 66:8319-26; PMID:16951136; http://dx.doi.org/10.1158/0008-5472.CAN-06-0410
18. Kang Y, Massagué J. Epithelial-mesenchymal transitions: twist in development and metastasis. Cell 2004; 118:277-9; PMID:15294153; http://dx.doi.org/10.1016/j.cell.2004.07.011
19. Howell GM, Grandis JR. Molecular mediators of metastasis in head and neck squamous cell carcinoma. Head Neck 2005; 27:710-7; PMID:15952195; http://dx.doi.org/10.1002/hed.20222
20. Leemans CR, Tiwari R, Nauta JJP, van der Waal I, Snow GB. Recurrence at the primary site in head and neck cancer and the significance of neck lymph node metastases as a prognostic factor. Cancer 1994; 73:187-90; PMID:8275423; http://dx.doi.org/10.1002/1097-0142(19940101)73:1<187::AID-CNCR2820730132>3.0.CO;2-J
21. Chua HH, Yeh TH, Wang YP, Huang YT, Sheen TS, Lo YC, Chou YC, Tsai CH. Upregulation of discoidin domain receptor 2 in nasopharyngeal carcinoma. Head Neck 2008; 30:427-36; PMID:18023033; http://dx.doi.org/10.1002/hed.20724
22 Luo R, Zhong B, Zong Y, Liang X, Wu Q, Lin S, He J, Liang Y, Li Z. The Constitutional Feature of Histopathological Types in Nasopharyngeal Carcinoma in High-incidence Area. Bulletin of Chinese Cancer 2001; 2001:473-5
23. Kawai I, Hisaki T, Sugiura K, Naito K, Kano K. Discoidin domain receptor 2 (DDR2) regulates proliferation of endochondral cells in mice. Biochem Biophys Res Commun 2012; 427:611-7; PMID:23022180; http://dx.doi.org/10.1016/j.bbrc.2012.09.106
24. Olaso E, Ikeda K, Eng FJ, Xu L, Wang LH, Lin HC, Friedman SL. DDR2 receptor promotes MMP-2-mediated proliferation and invasion by hepatic stellate cells. J Clin Invest 2001; 108:1369-78; PMID:11696582; http://dx.doi.org/10.1172/JCI200112373
25. Labrador JP, Azcoitia V, Tuckermann J, Lin C, Olaso E, Mañes S, Brückner K, Goergen JL, Lemke G, Yancopoulos G, et al. The collagen receptor DDR2 regulates proliferation and its elimination leads to dwarfism. EMBO Rep 2001; 2:446-52; PMID:11375938; http://dx.doi.org/10.1093/embo-reports/kve094
26. Olaso E, Labrador JP, Wang L, Ikeda K, Eng FJ, Klein R, Lovett DH, Lin HC, Friedman SL. Discoidin domain receptor 2 regulates fibroblast proliferation and migration through the extracellular matrix in association with transcriptional activation of matrix metalloproteinase-2. J Biol Chem 2002; 277:3606-13; PMID:11723120; http://dx.doi.org/10.1074/jbc.M107571200
27. Hou G, Wang D, Bendeck MP. Deletion of discoidin domain receptor 2 does not affect smooth muscle cell adhesion, migration, or proliferation in response to type I collagen. Cardiovasc Pathol 2012; 21:214-8; PMID:21865059; http://dx.doi.org/10.1016/j.carpath.2011.07.006
28. Kawata R, Shimada T, Maruyama S, Hisa Y, Takenaka H, Murakami Y. Enhanced production of matrix metalloproteinase-2 in human head and neck carcinomas is correlated with lymph node metastasis. Acta Otolaryngol 2002; 122:101-6; PMID:11876588; http://dx.doi.org/10.1080/00016480252775823
29. Kurahara S, Shinohara M, Ikebe T, Nakamura S, Beppu M, Hiraki A, Takeuchi H, Shirasuna K. Expression of MMPS, MT-MMP, and TIMPs in squamous cell carcinoma of the oral cavity: correlations with tumor invasion and metastasis. Head Neck 1999; 21:627-38; PMID:10487950; http://dx.doi.org/10.1002/(SICI)1097-0347(199910)21:7<627::AID-HED7>3.0.CO;2-2
30. O-Charoenrat P, Rhys-Evans PH, Eccles SA. Expression of matrix metalloproteinases and their inhibitors correlates with invasion and metastasis in squamous cell carcinoma of the head and neck. Arch Otolaryngol Head Neck Surg 2001; 127:813-20; PMID:11448356
31. Radhakrishnan R, Shrestha B, Bajracharya D. P31. Expression of matrix metalloproteinase-2 and tissue inhibitor of matrix metalloproteinase-2 in oral squamous cell carcinomas. Oral Oncol 2011; 47:S84; http://dx.doi.org/10.1016/j.oraloncology.2011.06.274
32. Fidler IJ. The pathogenesis of cancer metastasis: the 'seed and soil' hypothesis revisited. Nat Rev Cancer 2003; 3:453-8; PMID:12778135; http://dx.doi.org/10.1038/nrc1098
33. Gupta GP, Massagué J. Cancer metastasis: building a framework. Cell 2006; 127:679-95; PMID:17110329; http://dx.doi.org/10.1016/j.cell.2006.11.001
34. Yilmaz M, Christofori G. EMT, the cytoskeleton, and cancer cell invasion. Cancer Metastasis Rev 2009; 28:15-33; PMID:19169796; http://dx.doi.org/10.1007/s10555-008-9169-0
35. Hanahan D, Weinberg RA. Hallmarks of cancer: the next generation. Cell 2011; 144:646-74; PMID:21376230; http://dx.doi.org/10.1016/j.cell.2011.02.013
36. Thiery JP, Acloque H, Huang RYJ, Nieto MA. Epithelial-mesenchymal transitions in development and disease. Cell 2009; 139:871-90; PMID:19945376; http://dx.doi.org/10.1016/j.cell.2009.11.007
37. Sobin LH, Gospodarowicz MK, Wittekind C, eds. *TNM classification of malignant tumours*. Wiley. com, 2011.